On the Chemistry at Oxide/Water Interfaces: the Role of Interfacial Water

Mohammed Bin Jassar,[†] Qiwei Yao,[†] Flavio Siro Brigiano,[‡] Wanlin Chen,[*,¶] and Simone Pezzotti[*,†]

†*PASTEUR, Département de Chimie, École Normale Supérieure, PSL University, Sorbonne University, CNRS, 75005 Paris, France*

‡*Laboratoire de Chimie Theorique,Sorbonne Universite,UMR 7616, CNRS, 75005 Paris, France*

¶*Department of Physical Chemistry II, Ruhr University Bochum, D-44801 Bochum, Germany*

E-mail: wanlin.chen@ruhr-uni-bochum.de; simone.pezzotti@ens.psl.eu

Abstract

Oxide-water interfaces host many chemical reactions in nature and industry. There, reaction free energies markedly differ from bulk. While we can experimentally and theoretically measure these changes, we are often unable to address the fundamental question: what catalyses these reactions? Recent studies suggest that surface and electrostatics contributions are insufficient to answer. The interface modulates chemistry in subtle ways. Revealing them is essential to understanding interfacial reactions, hence improving industrial processes. Here, we introduce a thermodynamic approach combined with cavitation free energy analysis to disentangle the driving forces at play. We find water dictates chemistry via large variations of cavitation free energies across the interface. The resulting driving forces are both large enough to determine reaction output and highly tunable by adjusting interface composition, as showcased for silica-water interfaces. These findings shift the focus from common interpretations based on surface and electrostatics, and open exciting perspectives for regulating interfacial chemistry.

Introduction

Chemistry at oxide/water interfaces shapes our planet, due to the natural abundance of both oxides (silica, SiO_2, being the most abundant) and water.[1,2] It is also involved in a variety of industrial processes[3] (e.g., enhanced oil recovery,[4] renewable energy technologies,[5–8] photocatalysis,[9] heterogeneous catalysis,[10] drug delivery[2,11]), as well as speculated to have played an important role in the polymerization of amino acids for the formation of the first polypeptides on Earth.[12–16] Oxide/water interfaces exhibit fascinating catalytic properties, for instance, having lower kinetic barriers and shifting thermodynamic equilibria compared to what is known in bulk water.[1,13–18] Even reactions prohibited in bulk media were found favored at oxide/water interfaces, e.g. peptide-bond formation at silica/water[14–16,18,19] and synthesis of formic acid at MgO/water.[17] Understanding interfacial chemistry and its intricate connections to the molecular organization of both oxide surfaces and water at the interface is a challenge that continues to fascinate the scientific community across many fields, from electrochemistry to geochemistry and prebiotic chemistry, from theory to experiments.

At solid/liquid interfaces, specific interactions between reactive species and surface are the obvious candidates for dictating catalysis.[11,13,14,16,20–28] Their understanding has for instance propelled great progresses in the field of electro-catalysis, for assessing the performance of electrodes,[20–26] in the identification of chemical pathways relevant to the origin of life,[13,14,16] and in the design of mineral-based drug delivery systems in biomedicine.[11,27,28] These interactions dictate oxide chemistry in water vapor conditions, as suggested by experiments and by theoretical studies in the absence of (explicit) solvent. In these studies, inner-sphere chemistry is usually assumed, where the reaction is promoted by the direct bonding of the reactants to the surface.[29–34] When liquid water is put in contact with the oxide surface, both inner-sphere and outer-sphere reaction/adsorption, where all reactive species are separated from the surface by a water layer, are observed instead.[16,17,35–38] These findings suggest interfacial water plays a key but still unexplored role. The recent Molecular Dynamics (DFT-MD) simulation studies on peptide synthesis at silica/water[16] and formic

acid synthesis at MgO/water[17] are perfect examples of outer-sphere reactions, which are promoted at the interface, despite reactive species never interacting directly with the surface along the proposed reaction mechanisms.

If not direct solute-surface interactions, what catalyses these reactions? A possible answer is the strong local electric fields at play. They arise from the surface protonation state, adsorbed ions, and symmetry breaking within the H-bond network.[3,39–43] Electric fields can catalyze chemical reactions in liquid water and at interfaces by, e.g., inducing proton transfers,[44,45] tuning acid-base properties,[46] and promoting covalent bond breakage/formation.[47–50] Laporte at al.[17] investigated these effects at a MgO/water interface, by means of enhanced sampling techniques combined with DFT-MD simulations. They reported that the formation of formic acid is promoted by the local electric field. However, this was found to be only part of the answer: the electric field could only account for a part of the differences in the reaction free energy profiles computed at the interface and in the bulk.[17] Beyond surface and local electrostatics, the solvation of reactive species at the interface is expected to differ from bulk due to the restructuring of the water H-bond network close to the surface.[3,43,51–55] Despite this, when the coordination of the polar groups involved in the reaction was evaluated from MD simulations, such as in the glycine dimerization study of ref. 16, only little differences of a few H-bonds were found between interface and bulk. These differences were not sufficient by order of magnitude to explain the changes in reaction free energy (the free energy to break a H-Bond in liquid water is $\sim$0.5 kcal/mol,[17] while the free energy differences at play were on the order of several 10s of kJ/mol). Therefore, the interfacial water network must dictate chemistry in more subtle ways, beyond trivial solvation/desolvation effects.

Here, we propose a theoretical approach to quantitatively investigate the interfacial water contributions, by introducing a combination of two thermodynamic cycles, and cavitation free energy analysis from MD simulations. The method can be generally applied to any interfacial reaction. We showcase it for silica/water interfaces that have been extensively studied in

terms of both structure and reactivity.[1–3,11,39,43,52,54,56–58] We uncover the molecular origin of the interfacial water driving forces, and their decisive role in dictating reactivity.

Results and Discussions

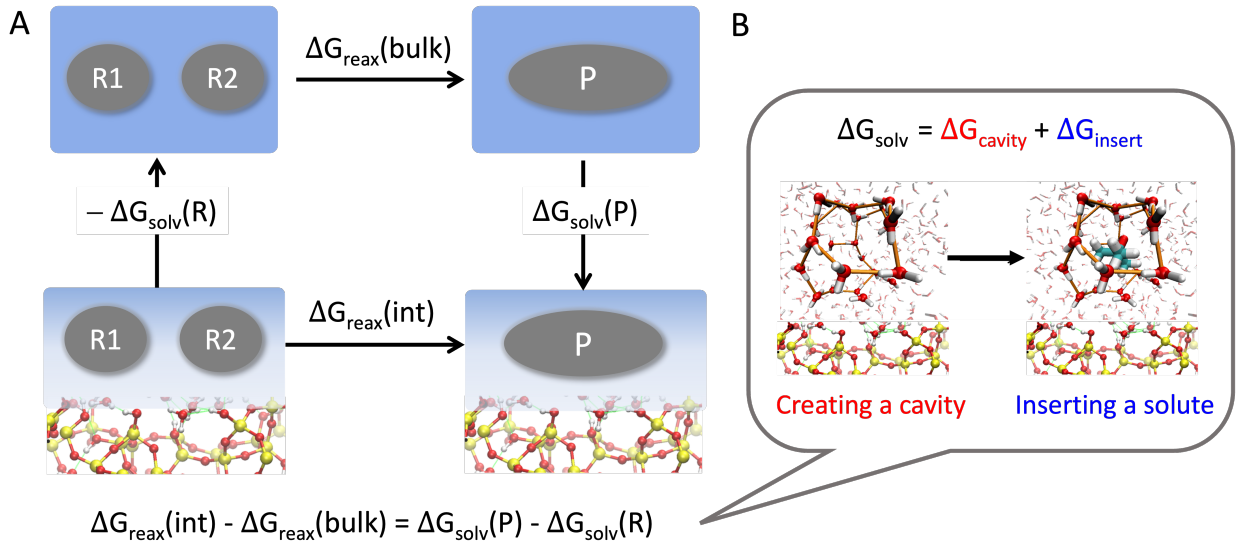

Figure 1: Two thermodynamic cycles are combined to spotlight the role of water in interfacial chemistry. (A) The first cycle (shown for a generic addition reaction) connects the reaction free energy at the interface, $\Delta G_{reax}(int)$, to that in the bulk ($\Delta G_{reax}(bulk)$). It interprets the effect of the interface on the reaction free energy ($\Delta G_{reax}(int) - \Delta G_{reax}(bulk)$) in terms of solvation (ΔG_{solv}) of reactants (R) and products (P) at interface *vs* in bulk. (B) The second cycle is illustrated for the solvation of an alcohol at a silica-water interface (the orange lines highlight the H-bonds between water molecules wrapped around the solute-cavity).[59] It decomposes ΔG_{solv} into contributions from cavity-formation (ΔG_{cavity}, which depends on interfacial *vs* bulk water network) and solute insertion (ΔG_{insert}, attractive interactions). ΔG_{solv}, ΔG_{cavity} and ΔG_{insert} are differences between interface and bulk. ΔG_{insert} contains all the contributions from surface, electrostatic and attractive solute-water interactions that have been evaluated so far. ΔG_{cavity} contains the role of interfacial water.

Thermodynamic approach to study the role of water. The effect of the interface on any reaction (or reaction step) is quantified by the difference in reaction free energy between two media: $\Delta G_{reax}(int) - \Delta G_{reax}(bulk)$. We connect interfacial and bulk chemistry with the thermodynamic cycle of Fig.1A. The cycle considers the alternative path where the

reactants move into the bulk, react there, and the products migrate back to the interface. This choice allows us to quantitatively interpret the effect of the interface on the reaction free energy in terms of its distinct solvation properties with respect to bulk:

$$\Delta G_{reax}(int) - \Delta G_{reax}(bulk) = \Delta G_{solv}(P) - \Delta G_{solv}(R) \quad (1)$$

where $\Delta G_{reax}(int)$ and $\Delta G_{reax}(bulk)$ can be theoretically predicted (together with a reaction mechanism) by DFT-MD simulations combined with enhanced sampling techniques. However, the various contributions giving rise to the difference between the two – contained in $\Delta G_{solv}(P)$ and $\Delta G_{solv}(R)$ (the differences in solvation free energy between interface and bulk) – cannot be disentangled by these calculations.

We adopt a second thermodynamic cycle (Fig.1B) to separate them in a step-wise manner.[59,60] It consists of two-steps where 1) the water H-bond network is perturbed to create a cavity that accommodates the solute; 2) the solute is inserted inside the cavity, switching on attractive interactions. The total solvation free energy changes from bulk to interface are given as the sum over these two steps: $\Delta G_{solv} = \Delta G_{cavity} + \Delta G_{insert}$ (where both ΔG_{cavity} and ΔG_{insert} are differences between interface and bulk). The contributions from surface, local fields, and attractive solute-water interactions that have been considered so far to rationalize chemistry at oxide/water interfaces are contained in ΔG_{insert}. ΔG_{cavity} quantifies the unexplored role of the water network.

ΔG_{cavity} (which encodes volume-exclusion effects, restructuring of the water network around the cavity, and surface desolvation upon solute binding)[59–63] does not depend on the nature of the solute, only on the solvent properties and the way they change close to the surface. It is readily computed from MD simulations by evaluating the statistics of water density fluctuations (i.e., the probability of spontaneously forming a cavity)[64,65] in the absence of any solute at the interface *vs* in bulk (see methods). Combining the two cycles

enables to quantify the interfacial water contribution to any chemical reaction (step):

$$\sum_{i=1}^{n_P} \Delta G_{cavity}(P_i) - \sum_{j=1}^{n_R} \Delta G_{cavity}(R_j) \quad (2)$$

where the i and j indexes run over the number of products (n_P) and reactants (n_R), respectively. The net contribution from attractive interactions (ΔG_{insert}) can then be quantified as the difference between the total reaction (step) free energy changes from bulk to interface from eq.1 and ΔG_{cavity} from eq.2 (calculated at the same level of theory). ΔG_{insert} becomes negligible in cases where only small changes are observed for the attractive interactions involving reactive species in going from bulk to interface. There, the catalytic effect of the interface must be searched in the water contribution, ΔG_{cavity}.

Water contributions to interfacial chemistry: ΔG_{cavity}. Is the water network responsible for the controversial balance of outer-sphere *vs* inner-sphere chemistry? In Fig.2A we quantify the contribution of ΔG_{cavity} to inner-sphere *vs* outer-sphere adsorption at a quartz (001)/water interface, for several species relevant for prebiotic chemistry, CO_2 reduction and geochemistry. To maintain the same level of theory as in recent DFT-MD studies,[16] we performed density fluctuation analysis from DFT-MD at the GGA level (see details in the method section). This level of theory provided a good description of the structure, spectroscopy, and acid-base properties of a diversity of silica/water interfaces (quartz and Amorphous, with different morphology, hydroxylation).[2,39,52,58,66] We find that ΔG_{cavity} systematically favors adsorption at the outer-sphere (by up to -5 k_BT, blue in Fig.2A), while disfavoring it (by +10 k_BT and more) at the inner-sphere. Molecules can hence undergo inner-sphere adsorption only if they form sufficiently strong interactions with the oxide to compensate the ΔG_{cavity} penalty. This result helps to understand why outer-sphere adsorption (and subsequent chemistry) was observed in previous studies on silica (and other oxides)/liquid water interfaces for the molecules shown in Fig.2A.[2,17,36,38,67] In the absence

of water, the ΔG_{cavity} penalty is missing, and the direct binding with the surface promotes inner-sphere adsorption.

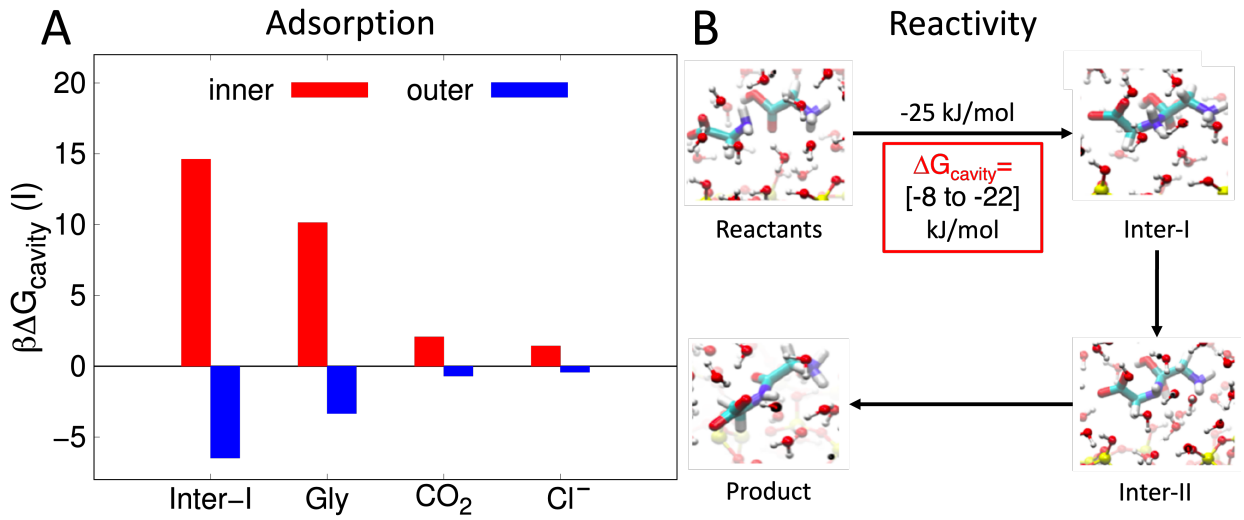

Figure 2: Interfacial water provides decisive ΔG_{cavity} contributions to: (A) Adsorption of reactive species at the interface. ΔG_{cavity} (in units of $k_BT = 1/\beta$) favors outer-sphere (in I2, blue) *vs* inner-sphere (in I1, red) adsorption (shown for several molecules at quartz(001)/water), therefore promoting outer-sphere chemistry. (B) Reaction free energies, shown for the outer-sphere reaction mechanism for glycine-glycine peptide formation from ref. 16. The first and rate determining step, the addition step to form Inter-I, was found favored at the interface by –25 kJ/mol; up to –22 kJ/mol are contributed by ΔG_{cavity}.

In Fig.2B, we investigate the role of water in reshaping reaction free energies at the interface. We consider the case of glycine dimerization, relevant in prebiotic chemistry. Outer-sphere adsorption and reaction of glycine at silica/water has been probed by NMR experiments[38] and computational studies.[16,36] The reaction mechanism of Fig.2B was proposed by DFT-MD metadynamics and shooting trajectories in ref. 16 (same simulation set-up as in the present work), with reactants, intermediates and products never forming direct interaction with the silica surface. The interface was found to decrease the free energy of the first and rate-determining step, i.e. the addition step between the two glycine to form inter-I, by -25 kJ/mol compared to the reaction in the bulk (and the reaction barrier

by -22 kJ/mol). This effect could not be explained in terms of surface and electrostatic contributions. We find that it can be rationalized by ΔG_{cavity}, which favors the formation of Inter-I from the two glycine by up to –22 kJ/mol. The 8–22 kJ/mol range is due to the high sensitivity of ΔG_{cavity} to the way the two reactive glycine approach each other (see Fig.S2 in SI, position and shape of reactants and inter-I cavities are given by metadynamics). The ΔG_{cavity} contribution is purely positional (vide infra), independent on the nature of glycine-water attractive interactions; that's why it remained elusive in previous studies. Since this reaction step has a late transition state,[16] we can speculate that the same mechanism also contributes in part to the lowering of the free energy barrier by -22 kJ/mol.

Identifying the molecular origin of these driving forces requires a detailed characterization of water density fluctuations at the interface. Fig. 3A shows $\Delta G_{cavity}(z)$ profiles for ellipsoidal cavities of decreasing volume (from blue to red). The shape is fixed to that of the cavity formed by a glycine molecule (see Fig.S3 in SI for analysis of different shapes). For all profiles, large $\Delta G_{cavity}(z)$ spatial variations are observed for z<4 Å (before bulk-like properties are recovered and $\Delta G_{cavity}(z) \simeq 0$) due to the specific molecular arrangement of water at the interface (MD-snapshot of Fig.3B). The strong binding of water molecules to the quartz surface, as confirmed by previous simulation and Sum Frequency Generation (SFG) studies,[3,41,56,58,66,69] leads to the formation of an ordered physisorbed water layer (I1 region, often denoted Binding Interfacial Layer, BIL).[66] Thanks to the good matching between the surface geometry (i.e. distance between surface SiOH groups) and the water-water H-bond pattern, BIL water molecules simultaneously maximize H-bonds with SiOH terminations as well as between themselves (see refs. 66 for more details). Hence, a large free energy cost is required for a solute to displace water molecules in I1 and arrive in direct contact with the surface. This disfavors inner-sphere adsorption. As a consequence of the in-plane ordering in I1, fewer inter-layer H-bond are formed between the BIL and the subsequent water layer, leading to an inter-layer I2 region (basically a water-water interface) where density fluctuations are enhanced and cavity formation becomes most favorable. The negative value

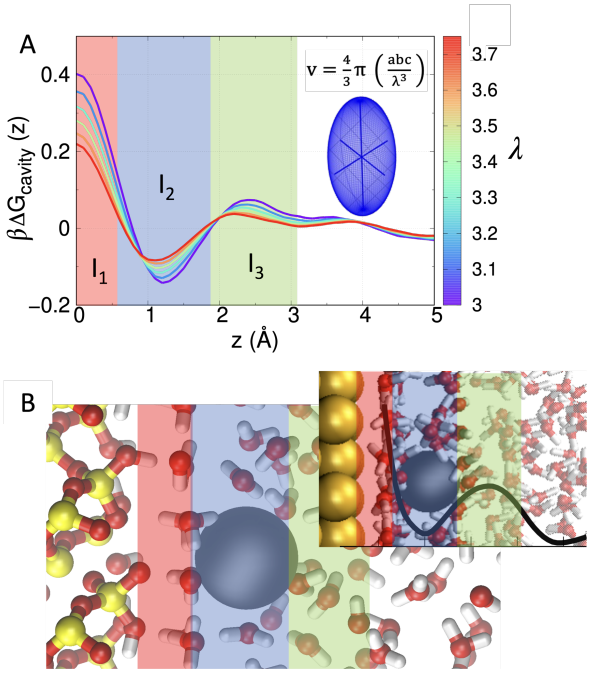

Figure 3: Water contributions to adsorption and reactivity are dictated by large ΔG_{cavity} spatial variations at the interfaces. (A) $\Delta G_{cavity}(z)$ profiles along the z-distance from the surface for ellipsoidal cavities with the shape of a glycine molecule at quartz (001)/water. From blue to red, the cavity volume is decreased by scaling the ellipsoid dimensions by λ. Large ΔG_{cavity} spatial variations are observed in the highlighted I1-3 interfacial regions. (B) MD-snapshot illustrating I1-3 at quartz (001)/water, including the ordered water layer that suppresses density fluctuations (hence disfavoring inner-sphere adsorption) in I1, as well as the water-water interface in I2, where density fluctuations are enhanced favoring cavity formation (grey sphere). The inset highlights the similarity with the same I1-3 regions at a previously studied gold/water interface.[65,68] The black curve is a typical $\Delta G_{cavity}(z)$ profile from ref. 65, showing large spatial variations as at quartz/water.

of $\Delta G_{cavity}(z)$ indicates that I2 is a preferential outer-sphere adsorption spot for hydrophobic/amphiphilic molecules: the cost to perturb the water network there is lower than in bulk water. Finally, an I3 region is identified in correspondence to the second interfacial water layer, where a small free energy cost (compared to bulk) has to be paid to access the "water-water interface" in I2. These results explain why ΔG_{cavity} promotes outer-sphere over inner-sphere adsorption.

Since $\Delta G_{cavity}(z)$ rapidly changes within a few Å , small variations in the volume, shape, and position of the cavities formed by reactive species can dramatically affect reaction free

energies at the interface, by changing the way the cavity volume is distributed among the I1-3 regions.[61,68] These effects give rise to the water network driving force to the peptide synthesis of Fig.2B: ΔG_{cavity} favors the reaction because the Inter-I cavity better fits within the I2 region, while one of the two glycine-cavities has to protrude into I3 (where cavity formation is disfavoured) when approaching the other. These positional effects increase the ΔG_{cavity} cost to solvate the reactants in the pre-reaction complex, while stabilizing their addition product, hence thermodynamically driving the reaction.

The stratification at the quartz (001)/water interface, with a first strongly bound water layer followed by a second weakly-bound one, is consistent with previous observations that the adsorption of the first water layer on the surface is much more exothermic than the subsequent adsorption of a second layer.[69] Moreover, the structure of the first water layer was found virtually unperturbed by the presence of the second layer, in agreement with our finding that BIL-water molecules dominant interactions are between themselves and with the quartz surface. The I1-3 regions at the quartz/water interface are reminiscent of that previously found at a gold/water interface[65,68] (inset of Fig.3B). There, in analogy with the present findings, density fluctuations are suppressed within the ordered water adlayer on top of the metal (I1), enhanced in the nearby water-water interface (I2), and reduced again in I3. Therefore, a common molecular origin exists for water network driving forces to the chemistry at the markedly different oxide/water and metal/water interfaces.

Effects of silica surface properties on ΔG_{cavity}. Can we exploit the ΔG_{cavity} driving forces to control interfacial chemistry? This depends on how much ΔG_{cavity} can be tuned by, e.g., adjusting the composition of both surface and liquid. For instance, based on the molecular understandings, we can imagine ΔG_{cavity} to correlate with surface hydrophilicity: the more the surface is hydrophilic, the more ordered the BIL, the larger the ΔG_{cavity} spatial variations at the interface. To test it, Fig.4 reports a case study of three surfaces of different morphology, crystallinity and hydroxylation: quartz(001) (Q/W interface, with

hydroxylation degree of 9.6 SiOH/nm^2)[66] and two amorphous silica models[2,52,70] with hydroxylation degrees of 4.5 SiOH/nm^2 (4.5/W, the experimental value obtained for several silica samples[71]) and 3.5 SiOH/nm^2 (3.5/W, representative of silica heat-treated at ∼570 K[2,52]). Surface hydrophilicity decreases from Q/W to 3.5/W.[2,52,66] As a measure of ΔG_{cavity} contributions to interfacial chemistry, Fig.4A displays the difference between ΔG_{cavity} for glycine outer- and inner-sphere adsorption, which is negative since ΔG_{cavity} favors outer-sphere adsorption (for all surfaces). An exceptional degree of tunability is found as a function of surface hydrophilicity: ΔG_{cavity} changes by almost an order of magnitude in going from Q/W to 3.5/W, with a difference of ∼13 k_BT (>30 kJ/mol).

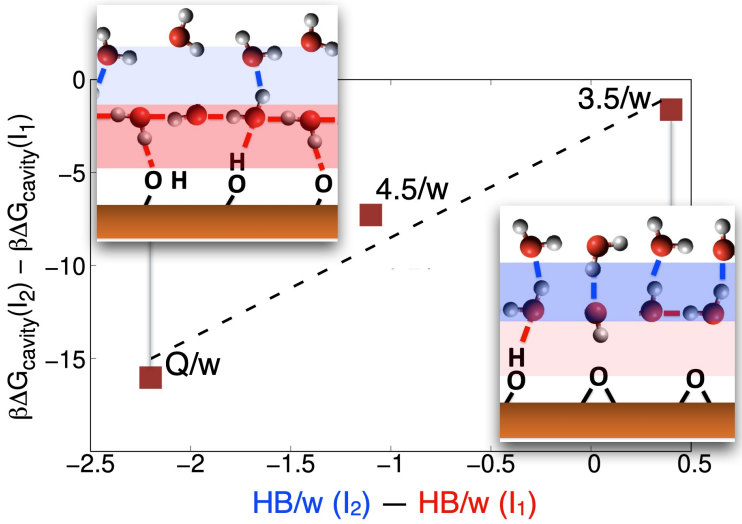

Figure 4: Surface modulations of ΔG_{cavity}. The difference between ΔG_{cavity} (in units of $k_BT = 1/\beta$) for glycine outer (I2)- *vs* inner-sphere (I1) adsorption for three silica/water interfaces (Q/w, 4.5/w, 3.5/w, as described in the text) is correlated with changes in the H-bond connectivity between I2 (blue in the schemes) and I1 (red in the schemes) regions, evaluated as the average number of H-bonds (blue and red solid lines in the schemes) per water molecule (HB/w) formed in I2 minus I1. The black dashed line is a guide to the eye, highlighting the correlation between ΔG_{cavity} driving force and interfacial structure. Large variations in both ΔG_{cavity} driving forces and H-bond connectivity at the interface are observed as a function of surface hydrophilicity, which decreases from Q/w to 3.5/w.

The free energy changes follow the degree of ordering induced by the silica surfaces within the BIL (I1), which in turn dictates H-bond connectivity in the inter-layer, I2 region (Fig.4B). As we learned from the ΔG_{cavity} difference between I1 and I2 at quartz/water, the higher the

H-bond connectivity within an interfacial region, the higher the free energy cost of cavity formation.[65,68] We quantify the connectivity in I2 minus I1 by calculating the average number of H-bonds per BIL water molecule (HB/w) in each region (including inter-layer H-bonds between BIL water and the adjacent water layer for I2, and intra-layer water-water and water-surface H-bonds for I1), and we correlate it with $\Delta G_{cavity}(outer) - \Delta G_{cavity}(inner)$. From the correlation of Fig.4, we propose the following mechanism for indirect surface modulations of ΔG_{cavity}: The more hydrophilic the surface, the higher the connectivity in I1 (red H-bonds in the scheme of Fig.4), the lower that in I2 (blue H-bonds). This, in turn, induces larger ΔG_{cavity} spatial variations at the interface (see Fig.S4 in SI) that enhance the water contribution to interfacial chemistry. As a perspective, both surface-water H-bonds that contribute to the connectivity in I1 and water-water H-bonds in I2 can be probed experimentally by, e.g., SFG spectroscopy in the OH-stretching region (they appear with a positive and negative sign in $\mathrm{Im}\chi^2$ spectra, respectively),[41,43,52,66] and by difference THz spectroscopy (water-water H-bonds by H-bond-stretching band and water-surface interaction by libration band).[53,59] This highlights a connection between spectroscopic and chemical properties of oxide/water interfaces, opening toward experimental characterizations of interfacial water driving forces.

Conclusions

In this work, we uncover the role of the water network in promoting chemistry at oxide/water interfaces. Strong surface-water interactions enhance water density fluctuations in a nearby water-water interface, giving rise to large spatial variations in the cavitation free energy (ΔG_{cavity}) within a few Å from the surface. These variations promote outer-sphere *vs* inner-sphere chemistry and are responsible for size, shape, and position effects on reaction-free energies. ΔG_{cavity} is found sufficiently large to regulate the adsorption of several classes of solutes (relevant for CO_2 reduction, prebiotic chemistry, geochemistry), as well as their

reactivity, as showcased for glycine dipeptide formation at a silica/water interface. This understanding opens opportunities for reaction steering, especially thanks to the high tunability of ΔG_{cavity} by adjusting surface and liquid composition, as we show for aqueous silica surfaces of varying hydrophilicity.

With the introduced theoretical approach, these opportunities can now be explored for any interfacial chemical reaction. Moreover, we find a correlation between ΔG_{cavity} and structural parameters (water-water and water-surface H-bonds) that can be experimentally measured by vibrational spectroscopies. We hope these findings will motivate further studies to explore the chemistry at oxide/water interfaces from the water perspective.

Methods

Born–Oppenheimer DFT-MD simulations of three silica-water interfaces were performed with CP2K/Quickstep,[72] PBE–D3,[73,74] GTH pseudopotentials,[75] and combined plane-wave (400 Ry cut-off) and DZVP-MOLOPT-SR basis sets. Simulation boxes are of 9.8 Å x 8.5 Å x 32 Å for Q/W, 13.4 Å x 13.3 Å x 37 Å for 4.5/W, and 12.67 Å x 13.27 Å x 37 Å for 3.5/W (same as in refs. 39,52,66, with amorphous slab models from ref. 70). Each simulation was performed in the NVT ensemble (with Nosé—Hoover thermostat,[76] T= 300 K, chain length= 3, time constant= 100 fs) for at least 160 ps, after 10 ps of equilibration.

Cavitation free energy profiles for the small cavities of Fig.3 were obtained by computing the probability ($P_{v,s}\ (0,z)$) that a cavity of volume (v), shape (s), and z-distance from the surface is spontaneously formed via water density fluctuations:[64,65]

$$P_{v,s}\ (0,z) = e^{-\beta\ \Delta\mu_{v,s}(z)} \tag{3}$$

$$\Delta G_{cavity}(z) = \ \Delta\mu^{int}_{v,s}\ (z) - \ \Delta\mu^{bulk}_{v,s} \tag{4}$$

where $\Delta\mu$ is the free energy cost of cavity formation, and $\beta = 1/\mathrm{k_B}T$. The statistics of DFT-MD is insufficient to compute $P_{v,s}\ (0,z)$ for large cavities, i.e., solutes in Fig.2. For

these, $\Delta G_{cavity}(z)$ is extrapolated with the recently introduced S.O.S. model of hydrophobic solvation[68] (see Fig.S1 in SI). The cavities were approximated to the smallest ellipsoidal void the solutes form in water (computed with respect to water oxygen centers, see Table S1 in SI).

Acknowledgement

This work is funded by the European Research Council (ERC, ELECTROPHOBIC, Grant Agreement No. 101077129). W.C. acknowledges the Alexander von Humboldt Foundation (AvH) for the research fellowship under the Henriette-Hertz-Scouting Program. This work was performed using HPC resources from GENCI. The authors thank Dr. Damien Laage and Miguel de la Puente (ENS, Paris) for stimulating discussions.

References

(1) Minakata, S.; Komatsu, M. Organic Reactions on Silica in Water. *Chem. Rev.* **2009**, *109*, 711–24.

(2) Rimola, A.; Costa, D.; Sodupe, M.; Lambert, J.-F.; Ugliengo, P. Silica surface features and their role in the adsorption of biomolecules: computational modeling and experiments. *Chem. Rev.* **2013**, *113*, 4216–4313.

(3) Bañuelos, J. L.; Borguet, E.; Brown Jr, G. E.; Cygan, R. T.; DeYoreo, J. J.; Dove, P. M.; Gaigeot, M.-P.; Geiger, F. M.; Gibbs, J. M.; Grassian, V. H.; others Oxide–and silicate–water interfaces and their roles in technology and the environment. *Chem. Rev.* **2023**, *123*, 6413–6544.

(4) Desmond, J. L.; Juhl, K.; Hassenkam, T.; Stipp, S. L. S.; Walsh, T. R.; Rodger, P. M. Organic-Silica Interactions in Saline: Elucidating the Structural Influence of Calcium in Low-Salinity Enhanced Oil Recovery. *Sci. Rep.* **2017**, *7*, 10944.

(5) Ko, S.; Han, X.; Shimada, T.; Takenaka, N.; Yamada, Y.; Yamada, A. Electrolyte design for lithium-ion batteries with a cobalt-free cathode and silicon oxide anode. *Nat. Sustain* **2023**, *6*, 1705–1714.

(6) Nong, H. N.; Falling, L. J.; Bergmann, A.; Klingenhof, M.; Tran, H. P.; Spöri, C.; Mom, R.; Timoshenko, J.; Zichittella, G.; Knop-Gericke, A.; others Key role of chemistry versus bias in electrocatalytic oxygen evolution. *Nature* **2020**, *587*, 408–413.

(7) Lian, Z.; Dattila, F.; López, N. Stability and lifetime of diffusion-trapped oxygen in oxide-derived copper CO2 reduction electrocatalysts. *Nat. Catal.* **2024**, 1–11.

(8) Albertini, P. P.; Newton, M. A.; Wang, M.; Segura Lecina, O.; Green, P. B.; Stoian, D. C.; Oveisi, E.; Loiudice, A.; Buonsanti, R. Hybrid oxide coatings generate stable Cu catalysts for CO2 electroreduction. *Nat. Mater.* **2024**, 1–8.

(9) Kruczynski, L.; Gesser, H. D.; Turner, C. W.; Speers, E. A. Porous titania glass as a photocatalyst for hydrogen production from water. *Nature* **1981**, *291*, 399–401.

(10) Kuai, L.; Chen, Z.; Liu, S.; Kan, E.; Yu, N.; Ren, Y.; Fang, C.; Li, X.; Li, Y.; Geng, B. Titania supported synergistic palladium single atoms and nanoparticles for room temperature ketone and aldehydes hydrogenation. *Nat. Commun.* **2020**, *11*, 48.

(11) Delle Piane, M.; Vaccari, S.; Corno, M.; Ugliengo, P. Silica-based materials as drug adsorbents: first principle investigation on the role of water microsolvation on ibuprofen adsorption. *J. Phys. Chem. A.* **2014**, *118*, 5801–5807.

(12) Ruiz-Mirazo, K.; Briones, C.; de la Escosura, A. Prebiotic Systems Chemistry: New Perspectives for the Origins of Life. *Chem. Rev.* **2014**, *114*, 285–366.

(13) Bujdák, J.; Rode, B. M. Glycine oligomerization on silica and alumina. *React. Kinet. Catal. Lett.* **1997**, *62*, 281–286.

(14) Lambert, J.-F.; Jaber, M.; Georgelin, T.; Stievano, L. A comparative study of the catalysis of peptide bond formation by oxide surfaces. *Phys. Chem. Chem. Phys.* **2013**, *15*, 13371–13380.

(15) Marshall-Bowman, K.; Ohara, S.; Sverjensky, D. A.; Hazen, R. M.; Cleaves, H. J. Catalytic peptide hydrolysis by mineral surface: Implications for prebiotic chemistry. *Geochim. Cosmochim. Acta* **2010**, *74*, 5852–5861.

(16) Siro Brigiano, F.; Gierada, M.; Tielens, F.; Pietrucci, F. Mechanism and Free-Energy Landscape of Peptide Bond Formation at the Silica–Water Interface. *ACS Catal.* **2022**, *12*, 2821–2830.

(17) Laporte, S.; Pietrucci, F.; Guyot, F.; Saitta, A. M. Formic Acid Synthesis in a Water–Mineral System: Major Role of the Interface. *J. Phys. Chem. C.* **2020**, *124*, 5125–5131.

(18) Lopes, I.; Piao, L.; Stievano, L.; Lambert, J.-F. Adsorption of amino acids on oxide supports: a solid-state NMR study of glycine adsorption on silica and alumina. *J. Phys. Chem. C.* **2009**, *113*, 18163–18172.

(19) Georgelin, T.; Jaber, M.; Bazzi, H.; Lambert, J.-F. Formation of activated biomolecules by condensation on mineral surfaces–a comparison of peptide bond formation and phosphate condensation. *Orig. Life Evol. Biosph.* **2013**, *43*, 429–443.

(20) Steinmann, S. N.; Michel, C. How to Gain Atomistic Insights on Reactions at the Water/Solid Interface? *ACS Catal.* **2022**, *12*, 6294–6301.

(21) Todorova, T. K.; Schreiber, M. W.; Fontecave, M. Mechanistic understanding of CO2 reduction reaction (CO2RR) toward multicarbon products by heterogeneous copper-based catalysts. *ACS Catal.* **2019**, *10*, 1754–1768.

(22) Feaster, J. T.; Shi, C.; Cave, E. R.; Hatsukade, T.; Abram, D. N.; Kuhl, K. P.; Hahn, C.; Nørskov, J. K.; Jaramillo, T. F. Understanding Selectivity for the Electrochemical Re-

duction of Carbon Dioxide to Formic Acid and Carbon Monoxide on Metal Electrodes. *ACS Catal.* **2017**, *7*, 4822–4827.

(23) Nilsson, A.; Pettersson, L.; Nørskov, J. *Chemical Bonding at Surfaces and Interfaces*; 2011.

(24) Abild-Pedersen, F.; Greeley, J.; Studt, F.; Rossmeisl, J.; Munter, T. R.; Moses, P. G.; Skúlason, E.; Bligaard, T.; Nørskov, J. K. Scaling Properties of Adsorption Energies for Hydrogen-Containing Molecules on Transition-Metal Surfaces. *Phys. Rev. Lett.* **2007**, *99*, 016105.

(25) Calle-Vallejo, F.; Martínez, J. I.; García-Lastra, J. M.; Rossmeisl, J.; Koper, M. T. M. Physical and Chemical Nature of the Scaling Relations between Adsorption Energies of Atoms on Metal Surfaces. *Phys. Rev. Lett.* **2012**, *108*, 116103.

(26) Luo, F. et al. P-block single-metal-site tin/nitrogen-doped carbon fuel cell cathode catalyst for oxygen reduction reaction. *Nat. Mater.* **2020**, *19*, 1215–1223.

(27) Delle Piane, M.; Corno, M. Can Mesoporous Silica Speed Up Degradation of Benzodiazepines? Hints from Quantum Mechanical Investigations. *Materials* **2022**, *15*, 1357.

(28) Makila, E.; Kivela, H.; Shrestha, N.; Correia, A.; Kaasalainen, M.; Kukk, E.; Hirvonen, J.; Santos, H. A.; Salonen, J. Influence of surface chemistry on ibuprofen adsorption and confinement in mesoporous silicon microparticles. *Langmuir* **2016**, *32*, 13020–13029.

(29) Rimola, A.; Ugliengo, P.; Sodupe, M. Formation versus hydrolysis of the peptide bond from a quantum-mechanical viewpoint: the role of mineral surfaces and implications for the origin of life. *Int. J. Mol. Sci.* **2009**, *10*, 746–760.

(30) Rimola, A.; Sodupe, M.; Ugliengo, P. Amide and peptide bond formation: Interplay

between strained ring defects and silanol groups at amorphous silica surfaces. *J. Phys. Chem. C.* **2016**, *120*, 24817–24826.

(31) Rimola, A.; Tosoni, S.; Sodupe, M.; Ugliengo, P. Does Silica Surface Catalyse Peptide Bond Formation? New Insights from First-Principles Calculations. *ChemPhysChem* **2006**, *7*, 157–163.

(32) Rimola, A.; Fabbiani, M.; Sodupe, M.; Ugliengo, P.; Martra, G. How does silica catalyze the amide bond formation under dry conditions? Role of specific surface silanol pairs. *ACS Catal.* **2018**, *8*, 4558–4568.

(33) Pantaleone, S.; Ugliengo, P.; Sodupe, M.; Rimola, A. When the Surface Matters: Prebiotic Peptide-Bond Formation on the TiO2 (101) Anatase Surface through Periodic DFT-D2 Simulations. *Chem. Eur. J.* **2018**, *24*, 16292–16301.

(34) El Samrout, O.; Fabbiani, M.; Berlier, G.; Lambert, J.-F.; Martra, G. Emergence of Order in Origin-of-Life Scenarios on Mineral Surfaces: Polyglycine Chains on Silica. *Langmuir* **2022**, *38*, 15516–15525.

(35) Ben Shir, I.; Kababya, S.; Schmidt, A. Binding specificity of amino acids to amorphous silica surfaces: solid-state NMR of glycine on SBA-15. *J. Phys. Chem. C.* **2012**, *116*, 9691–9702.

(36) Rimola, A.; Civalleri, B.; Ugliengo, P. Neutral vs zwitterionic glycine forms at the water/silica interface: structure, energies, and vibrational features from B3LYP periodic simulations. *Langmuir* **2008**, *24*, 14027–14034.

(37) Nonella, M.; Seeger, S. Investigating alanine–silica Interaction by means of first-principles molecular-dynamics simulations. *ChemPhysChem* **2008**, *9*, 414–421.

(38) Ben Shir, I.; Kababya, S.; Amitay-Rosen, T.; Balazs, Y. S.; Schmidt, A. Molecular level

characterization of the inorganic- bioorganic interface by solid state NMR: Alanine on a silica surface, a case study. *J. Phys. Chem. B.* **2010**, *114*, 5989–5996.

(39) Tuladhar, A.; Dewan, S.; Pezzotti, S.; Siro Brigiano, F.; Creazzo, F.; Gaigeot, M.-P.; Borguet, E. Ions Tune Interfacial Water Structure and Modulate Hydrophobic Interactions at Silica Surfaces. *J. Am. Chem. Soc.* **2020**, *142*.

(40) Ohno, P. E.; Saslow, S. A.; fei Wang, H.; Geiger, F. M.; Eisenthal, K. B. Phase-referenced nonlinear Spectroscopy of the alpha-quartz/water Interface. *Nat. Comm.* **2016**, *7*, 13587–13591.

(41) Wang, H.; Xu, Q.; Liu, Z.; Tang, Y.; Wei, G.; Shen, Y. R.; Liu, W.-T. Gate-controlled sum-frequency vibrational spectroscopy for probing charged oxide/water interfaces. *J. Phys. Chem. Lett.* **2019**, *10*, 5943–5948.

(42) Rehl, B.; Ma, E.; Parshotam, S.; DeWalt-Kerian, E. L.; Liu, T.; Geiger, F. M.; Gibbs, J. M. Water structure in the electrical double layer and the contributions to the total interfacial potential at different surface charge densities. *J. Am. Chem. Soc.* **2022**, *144*, 16338–16349.

(43) Gonella, G.; Backus, E. H.; Nagata, Y.; Bonthuis, D. J.; Loche, P.; Schlaich, A.; Netz, R. R.; Kühnle, A.; McCrum, I. T.; Koper, M. T.; others Water at charged interfaces. *Nat. Rev. Chem.* **2021**, *5*, 466–485.

(44) Saitta, A. M.; Saija, F.; Giaquinta, P. V. Ab initio molecular dynamics study of dissociation of water under an electric field. *Phys. Rev. Lett.* **2012**, *108*, 207801.

(45) Cassone, G. Nuclear quantum effects largely influence molecular dissociation and proton transfer in liquid water under an electric field. *J. Phys. Chem. Lett.* **2020**, *11*, 8983–8988.

(46) Murke, S.; Chen, W.; Pezzotti, S.; Havenith, M. Tuning Acid–Base Chemistry at an Electrified Gold/Water Interface. *J. Am. Chem. Soc.* **2024**,

(47) Vaissier, V.; Sharma, S.; Schaettle, K.; Zhang, T.; Head-Gordon, T. Computational Optimization of Electric Fields for Improving Catalysis of a Designed Kemp Eliminase. *ACS Catal.* **2018**, *8*, 219–227.

(48) Welborn, V. V.; Head-Gordon, T. Fluctuations of Electric Fields in the Active Site of the Enzyme Ketosteroid Isomerase. *J Am Chem Soc* **2019**, *141*, 12487–12492.

(49) Cassone, G.; Sponer, J.; Sponer, J. E.; Pietrucci, F.; Saitta, A. M.; Saija, F. Synthesis of (d)-erythrose from glycolaldehyde aqueous solutions under electric field. *Chem. Commun.* **2018**, *54*, 3211–3214.

(50) Cassone, G.; Pietrucci, F.; Saija, F.; Guyot, F.; Saitta, A. M. One-step electric-field driven methane and formaldehyde synthesis from liquid methanol. *Chem. Sci.* **2017**, *8*, 2329–2336.

(51) Du, Q.; Freysz, E.; Shen, Y. R. Surface vibrational spectroscopic studies of hydrogen bonding and hydrophobicity. *Science* **1994**, *264*, 826–828.

(52) Cyran, J. D.; Donovan, M. A.; Vollmer, D.; Brigiano, F. S.; Pezzotti, S.; Galimberti, D. R.; Gaigeot, M.-P.; Bonn, M.; Backus, E. H. G. Molecular hydrophobicity at a macroscopically hydrophilic surface. *Proc. Natl. Acad. Sci. U.S.A.* **2019**, *116*, 1520–1525.

(53) Pezzotti, S.; Serva, A.; Sebastiani, F.; Brigiano, F. S.; Galimberti, D. R.; Potier, L.; Alfarano, S.; Schwaab, G.; Havenith, M.; Gaigeot, M.-P. Molecular fingerprints of hydrophobicity at aqueous interfaces from theory and vibrational spectroscopies. *J. Phys. Chem. Lett.* **2021**, *12*, 3827–3836.

(54) Hassanali, A. A.; Singer, S. J. Model for the water- amorphous silica interface: the undissociated surface. *J. Phys. Chem. B.* **2007**, *111*, 11181–11193.

(55) Piontek, S. M.; Borguet, E. Vibrational Dynamics at Aqueous–Mineral Interfaces. *J. Phys. Chem. C.* **2022**, *126*, 2307–2324.

(56) Liu, W.-T.; Shen, Y. Surface vibrational modes of α-quartz (0001) probed by sum-frequency spectroscopy. *Phys. Rev. Lett.* **2008**, *101*, 016101.

(57) Lunt, A. J. G.; Chater, P.; Korsunsky, A. M. On the origins of strain inhomogeneity in amorphous materials. *Sci. Rep.* **2018**, *8*, 1574.

(58) Sulpizi, M.; Gaigeot, M.-P.; Sprik, M. The silica–water interface: how the silanols determine the surface acidity and modulate the water properties. *J. Comput. Chem.* **2012**, *8*, 1037–1047.

(59) Pezzotti, S.; Sebastiani, F.; van Dam, E. P.; Ramos, S.; Conti Nibali, V.; Schwaab, G.; Havenith, M. Spectroscopic fingerprints of cavity formation and solute insertion as a measure of hydration entropic loss and enthalpic gain. *Angew. Chem. Int. Ed.* **2022**, *134*, e202203893.

(60) Chandler, D. Interfaces and the driving force of hydrophobic assembly. *Nature* **2005**, *437*, 640–647.

(61) Serva, A.; Havenith, M.; Pezzotti, S. The role of hydrophobic hydration in the free energy of chemical reactions at the gold/water interface: Size and position effects. *J. Chem. Phys.* **2021**, *155*, 204706.

(62) Lum, K.; Chandler, D.; Weeks, J. D. Hydrophobicity at Small and Large Length Scales. *J. Phys. Chem. B* **1999**, *103*, 4570–4577.

(63) Eggert, T.; Hörmann, N. G.; Reuter, K. Cavity formation at metal–water interfaces. *J. Chem. Phys.* **2023**, *159*.

(64) Limmer, D. T.; Willard, A. P.; Madden, P.; Chandler, D. Hydration of metal surfaces can be dynamically heterogeneous and hydrophobic. *Proc. Natl. Acad. Sci. U.S.A.* **2013**, *110*, 4200–4205.

(65) Serva, A.; Salanne, M.; Havenith, M.; Pezzotti, S. Size dependence of hydrophobic hydration at electrified gold/water interfaces. *Proc. Natl. Acad. Sci. U.S.A.* **2021**, *118*, e2023867118.

(66) Pezzotti, S.; Galimberti, D. R.; Gaigeot, M.-P. Deconvolution of BIL-SFG and DL-SFG spectroscopic signals reveals order/disorder of water at the elusive aqueous silica interface. *Phys. Chem. Chem. Phys.* **2019**, *21*, 22188–22202.

(67) Pfeiffer-Laplaud, M.; Gaigeot, M.-P. Electrolytes at the Hydroxylated (0001) α-Quartz/Water Interface: Location and Structural Effects on Interfacial Silanols by DFT-Based MD. *J. Phys. Chem. C* **2016**, *120*, 14034–14047.

(68) Serva, A.; Pezzotti, S. S.O.S: Shape, orientation, and size tune solvation in electrocatalysis. *J. Chem. Phys.* **2024**, *160*, 094707.

(69) Chen, Y.-W.; Chu, I.-H.; Wang, Y.; Cheng, H.-P. Water thin film-silica interaction on α-quartz (0001) surfaces. *Phys. Rev. B* **2011**, *84*, 155444.

(70) Ugliengo, P.; Sodupe, M.; Musso, F.; Bush, I.; Orlando, R.; Dovesi, R. Realistic models of hydroxylated amorphous silica surfaces and MCM-41 mesoporous material simulated by large-scale periodic B3LYP calculations. *Adv. Mater.* **2008**, *20*, 4579–4583.

(71) Zhuravlev, L. The surface chemistry of amorphous silica. Zhuravlev model. *Colloids Surf. A Physicochem. Eng. Asp.* **2000**, *173*, 1–38.

(72) VandeVondele, J.; Krack, M.; Mohamed, F.; Parrinello, M.; Chassaing, T.; Hutter, J. Quickstep: Fast and Accurate Density Functional Calculations Using a Mixed Gaussian and Plane Waves Approach. *Comp. Phys. Comm.* **2005**, *167*, 103–128.

(73) Perdew, J. P.; Burke, K.; Ernzerhof, M. Generalized Gradient Approximation Made Simple. *Phys. Rev. Lett.* **1996**, *77*, 3865–3868.

(74) Grimme, S.; Ehrlich, S.; Goerigk, L. Effect of the Damping Function in Dispersion Corrected Density Functional Theory. *J. Comput. Chem.* **2011**, *32*, 1456–1465.

(75) Goedecker, S.; Teter, M.; Hutter, J. Separable Dual-Space Gaussian Pseudopotentials. *Phys. Rev. B* **1996**, *54*, 1703–1710.

(76) Nosé, S. Molecular Physics : An International Journal at the Interface Between Chemistry and Physics. A Molecular Dynamics Study of Polarizable Water. *Mol. Phys.* **2006**, *52*, 255–268.